catalysts

MDPI

Article

Comparative Analysis of G-Quadruplex DNAzyme Scaffolds and Split Modes for Programmable Biosensing

Dunsin S. Osalaye [1], Raphael I. Adeoye [2], Sylvia O. Malomo [1] and Femi J. Olorunniji [2,*]

[1] Department of Biochemistry, Faculty of Life Sciences, University of Ilorin, Ilorin P.M.B. 1515, Nigeria
[2] School of Pharmacy & Biomolecular Sciences, Faculty of Health, Innovation, Technology and Science, Liverpool John Moores University, Liverpool L3 3AF, UK
* Correspondence: f.j.olorunniji@ljmu.ac.uk

Abstract

G-quadruplex (G4) DNAzymes, guanine-rich sequences that fold into four-stranded structures and bind hemin to mimic peroxidase activity, are widely used in biosensing. Split G4 DNAzymes offer conditional activation upon target recognition, enabling high specificity and modularity. However, achieving low OFF-state leakage remains a major challenge. Here, we systematically characterized four representative G4 scaffolds, C-myc, Bcl2, PS5.M, and C-kit, under standardized ABTS/H_2O_2 conditions to assess their kinetic properties and suitability for split designs. C-myc exhibited the highest sustained activity and near-linear concentration dependence, making it ideal for quantitative sensing, while Bcl2 showed durable catalysis suited for extended read windows. C-kit produced rapid bursts with early plateaus, favoring binary outputs, and PS5.M initiated quickly but inactivated rapidly, suggesting potential application of systems requiring fast response. Split-mode analysis revealed that symmetric 2:2 partitions often retained significant activity, whereas asymmetric 3:1 splits reduced but did not eliminate leakage. Among the four G4 DNAzymes, PS5.M demonstrated the most promising OFF-state suppression. Design strategies to minimize leakage including non-classical splits, loop/flank edits, and template-assisted assembly could be used to optimize biosensor functionalities. These findings identify essential factors critical for designing robust split DNAzyme biosensors, advancing applications in diagnostics and molecular logic gates.

Keywords: G-quadruplex DNAzyme; split DNAzyme biosensor; kinetic characterization; signal-to-background ratio; non-classical split design

Academic Editors: Teodora Bavaro and Marina Simona Robescu

Received: 21 November 2025
Revised: 21 December 2025
Accepted: 26 December 2025
Published: 30 December 2025

1. Introduction

DNA nanotechnology has transformed biosensing by introducing programmable molecular systems for sensitive and specific detection of biomolecules. Among these, G-quadruplex (G4) DNAzymes, guanine-rich sequences that fold into four-stranded structures, stand out as versatile catalytic entities. When complexed with hemin, these structures mimic peroxidase activity, catalyzing H_2O_2-mediated oxidation of chromogenic substrates such as ABTS, producing measurable colorimetric signals [1–3]. Their small size, robustness, and tunable architecture make them attractive signal transducers in bioanalysis.

A particularly innovative adaptation is the split G-quadruplex DNAzyme, which enables conditional assembly of the active structure in response to target recognition. In these systems, a G-rich sequence is divided into two or more fragments that reassemble into a functional G4 only upon hybridization with a complementary target strand (Figure 1).

This design enhances specificity and modularity, allowing integration into logic-gated architectures for multiplexed detection [4,5]. Upon target-induced reconstitution, the G4 binds hemin to form a DNAzyme capable of catalyzing oxidative reactions, yielding a detectable signal.

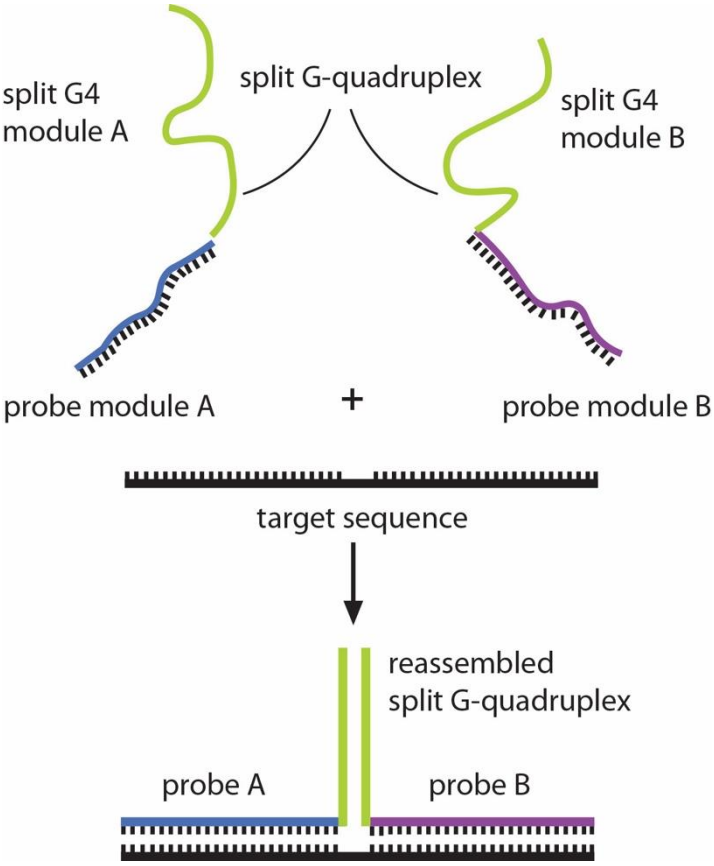

Figure 1. Template-directed assembly of split G-quadruplex-hemin DNAzyme. The G-quadruplex DNA sequence (green) is split into two modules (A and B) and attached to two probe sequences (probe module A and probe module B. Recognition and hybridization of the probe modules to the complementary target DNA results in the reassembly of the split G4 modules to form a functional split G-quadruplex DNAzyme with peroxidase activity.

Despite their promise, challenges remain in optimizing the folding topology and catalytic efficiency of split G4 DNAzymes. Hemin–G4 complexes rely on stacking interactions at exposed terminal G-quartets, with catalytic performance strongly influenced by G4 topology (parallel vs. non-parallel), terminal tetrad accessibility, loop composition, and flanking nucleotides [2,3,6]. Parallel topologies and engineered 3′ environments such as adjacent adenines generally enhance activity. Strategies to improve performance include proximity-driven multimerization, covalent hemin–G4 integration, and loop engineering [7–9].

Split DNAzyme design principles emphasize minimizing OFF-state activity while enabling efficient ON-state assembly. Split G-quadruplex DNAzyme designs typically use two classical strategies: 2:2 or 3:1 splits, referring to how guanine tracts are distributed between strands. In a 2:2 split, each fragment contributes two G-runs; for example, 5′-GGG TGGG AGGG CGGG-3′ can be divided into 5′-GGG TGGG-3′ and 5′-AGGG CGGG-3′. Upon target binding, these strands reassemble into a functional G4, activating peroxidase-like activity. In a 3:1 split, one fragment carries three G-runs and the other a single tract, reducing spontaneous folding and background leakage. While asymmetric splits enhance selectivity, symmetric splits often yield more stable reconstituted structures. Both strate-

gies underpin conditional activation in biosensors, enabling target-driven assembly of G4/hemin complexes for sensitive and specific detection. Non-classical splits that partition G-tracts or introduce destabilizing edits further suppress spontaneous folding [4]. Successful designs balance structural integrity for target-induced assembly with OFF-state silence, a prerequisite for high signal-to-background ratios.

Several well-characterized sequences serve as models for G4-based biosensors: C-myc (5′-GAGGGTGGGGAGGGTGGGGAAG-3′) and C-kit (5′-CGGGCGGGCGCGAGGGAGGGG-3′) adopt parallel G4s in K^+, showing strong peroxidase activity and robustness across conditions [5,10]. Bcl2 (5′-GGGCGCGGGAGGAAGGGGGCGGG-3′), derived from a promoter region, forms hybrid or parallel folds but assembles into a uni-parallel G4 upon hemin binding, exhibiting durable catalytic activity [11]. PS5.M (5′-GTGGGTCATTGTGGGTGGGTGTGG-3′), a classical SELEX product, favors non-parallel structures and shows moderate activity, which can be enhanced by additives or topology-modifying conditions [7]. These scaffolds differ in loop architecture, tract distribution, and folding stability, features that influence both intact DNAzyme kinetics and tolerance to fragmentation. For biosensing, desirable attributes include rapid signal onset, linear response with catalyst dose, and minimal leakage upon splitting.

This work addresses two key questions for rational biosensor design: (i) Do commonly used G4 scaffolds exhibit kinetic properties suitable for biosensing? To address this, we compared the catalytic performance of C-myc, Bcl2, PS5.M, and C-kit under standardized ABTS/H_2O_2 conditions to identify sequences suited for quantitative assays or rapid yes/no formats. (ii) Can these scaffolds be effectively split into catalytically silent fragments? We evaluate two split strategies, 2:2 (symmetric) and 3:1 (asymmetric), for each sequence, assessing OFF-state leakage and identifying configurations that meet the criterion of near-zero fragment activity.

Our findings reveal distinct kinetic signatures and split behaviors. C-myc delivers the highest sustained activity and near-linear concentration response, making it ideal for quantitative sensing. Bcl2 exhibits slower initial rates but durable catalysis, suitable for extended read windows. C-kit shows a rapid burst followed by early plateau, favoring quick true/false formats, while PS5.M initiates fast but inactivates quickly, suggesting utility for rapid triggers. Split-mode analysis demonstrates that PS5.M offers the most favorable OFF-state suppression among the set we investigated.

This study provides a systematic, side-by-side evaluation of both intact and split G-quadruplex DNAzymes under standardized conditions, linking kinetic performance to known structural features of the intact G4-DNAzymes. By integrating quantitative activity profiling with leakage analysis, we establish design principles for selecting scaffolds and optimizing split strategies to achieve high ON/OFF ratios. These insights address a critical gap in the rational engineering of split DNAzyme biosensors, enabling more reliable, modular, and application-specific platforms for diagnostics and molecular logic. Our findings lay the groundwork for next-generation nucleic acid-based sensors with improved sensitivity, specificity, and programmability.

2. Results

We started by comparing the peroxidase activities of four G-rich promoter-derived DNAzymes (BCl2, C-myc, PS5.M, and C-kit) each tested at three DNA concentrations with 5 mM H_2O_2/1 mM ABTS (Figure 2). Triplicate time courses (0–600 s) at 0.01, 0.025, and 0.05 μM were analyzed after time-matched baseline subtraction using hemin-only controls. Initial rates were obtained by linear regression over 0–120 s. Final net absorbance at 600 s and time-to-half-maximum (T_{50}) were also calculated (Table 1).

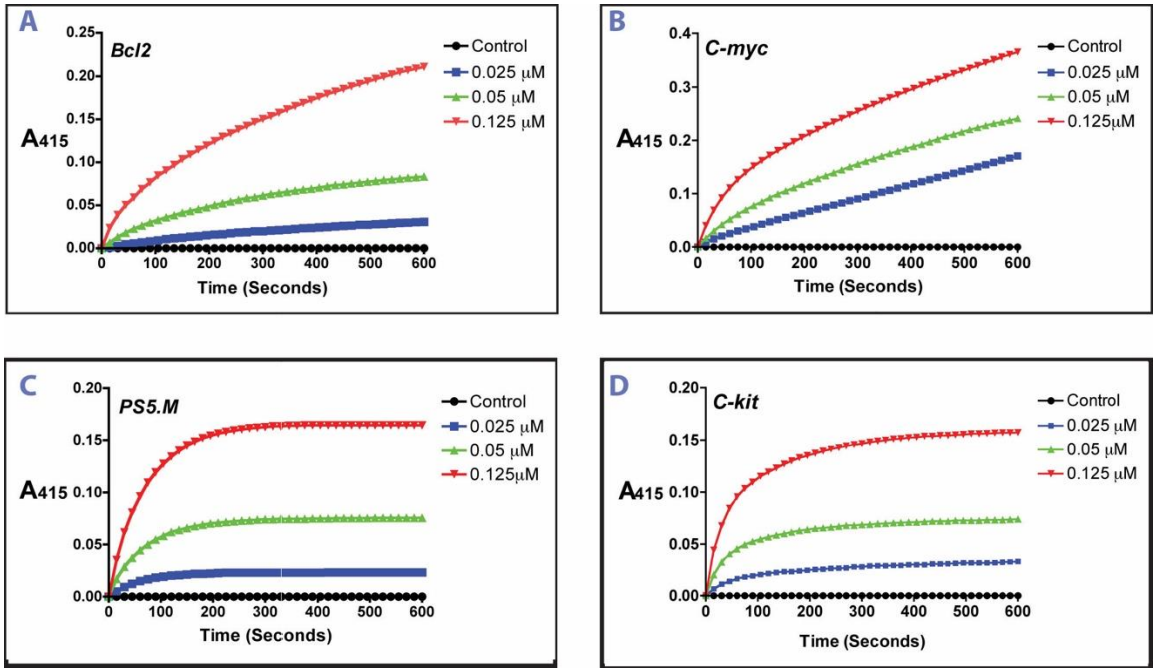

Figure 2. Peroxidase activities of Bcl2 (**A**), C-myc (**B**), PS5.M (**C**), and C-kit (**D**) G-quadruplex DNAzymes. Catalytic activities were determined at 25 °C using ABTS/H_2O_2 oxidation. DNAzyme activities were determined at 0.025, 0.05, and 0.125 μM DNA complexed using 1 mM ABTS, and 5 mM H_2O_2 as described in the Methodology section. Absorbance at 415 nm (A_{415}) was monitored every 5 s for 600 s. Control reactions contain 1 μM hemin in place of the DNA/hemin complex.

Table 1. Initial rates, V_o (Abs s^{-1}), and endpoint activities (at 600 s) at 0.125 μM DNAzyme.

G4/Hemin	V_o (Abs/s) ($\times 10^{-3}$)	A_{415} (600 s)	T_{50} (s)
C-myc	1.289 ± 0.059	0.365 ± 0.025	152 ± 7
PS5.M	1.066 ± 0.031	0.164 ± 0.006	46 ± 3
c-Kit	8.82 ± 0.220	0.157 ± 0.007	40 ± 2
Bcl2	7.11 ± 0.390	0.211 ± 0.005	155 ± 5

Initial rates (expressed as Vo, Abs/s) were obtained by linear regression over 0–120 s of the time course. Final net absorbance at 600 s at 0.125 μM DNAzyme was taken as the endpoint and T_{50} was calculated as the time to reach half-maximum. Each datum represents mean ± standard deviation from three replicate experiments.

2.1. Overall Activities of G4-Quadruplex DNAzymes and Concentration Dependence

All four G4/hemin complexes exhibited clear ABTS oxidation above the no-DNA control across the timescale of 600 s, with the magnitude of A_{415} increasing linearly with catalyst concentration. This concentration dependence was most linear and sustained for C-myc and Bcl2 (near-proportional separation of traces), whereas PS5.M and C-kit showed early rapid increases followed by pronounced plateaus, yielding sub-linear gains at higher concentration by 600 s.

As summarized in Table 1, at 0.125 μM, the mean initial rates (Abs s^{-1}) were as follows: C-myc 1.289×10^{-3}; PS5.M 1.066×10^{-3}; c-Kit 8.82×10^{-4}; Bcl2 7.11×10^{-4}. Final A_{600} at 600 s (net): C-myc 0.365; Bcl2 0.211; PS5.M 0.164; c-Kit 0.157. T_{50} (s) at 0.125 μM: c-Kit 40; PS5.M 46; C-myc 152; Bcl2 155.

The endpoint activities at 600 s and 0.125 μM DNAzyme concentration follow the trend C-myc ≫ Bcl2 > PS5.M ≈ C-kit, while the initial phase (first 30–100 s at 0.125 μM) shows PS5.M ≳ C-kit > C-myc > Bcl2. These trends suggest that C-myc and Bcl2 may maintain catalytically competent complexes over longer times, while PS5.M and C-kit display burst-like kinetics that could indicate fast activation followed by partial inactivation or saturation. While such time-dependent attenuation is well documented for hemin/G4 DNAzymes

under peroxidative conditions [12], more precise experimental analyses are required to reach definite conclusion on these observations.

2.2. Sequence-Specific Peroxidase Activities of G-Quadruplex DNAzymes

C-myc: The kinetic pattern shows activities rise rapidly and continue quasi-linearly to the end of the recording without obvious saturation, producing the highest endpoint absorbances at all three concentrations studied. This is consistent with the parallel, propeller-type C-myc G4 that presents an accessible terminal G-tetrad for 3′-end hemin stacking known to perform better than antiparallel ones. Moreover, multimerization of parallel scaffolds such as C-myc tends to show synergistic rate enhancement, reinforcing their suitability for signal amplification designs [7,10,13].

Bcl2: The initial slope is more modest than for C-myc, but activity persists throughout 600 s and the endpoint surpasses PS5.M and C-kit at comparable loadings. Bcl-2 promoter G4s can populate hybrid forms, yet hemin binding drives a uni-parallel conformation with peroxidase activity in agreement with the sustained catalytic activity observed here [11].

PS5.M: The kinetic pattern displays a fast burst (steep early slope) followed by a clear saturation by approximately 200–300 s, even at low DNAzyme concentrations. PS5.M originates from *in vitro* selection for porphyrin metallation (not peroxidation) and frequently adopts non-parallel folds. Such topologies and loop arrangements can support high initial activity but are more likely to undergo inactivation or adopt less favorable stable hemin stacking in ABTS/H_2O_2 assays. This pattern of results is consistent with observations that shifting non-parallel G4s toward parallel (e.g., with polyamines like spermine) increases peroxidase output [14,15].

C-kit: Similar to PS5.M, C-kit shows a rapid rise then a plateau, giving endpoints close to PS5.M at 0.125 μM. Crystallographic and NMR work on C-kit promoter sequences (kit1/kit2) reveals stable parallel folds with short loops, or, in some contexts, alternative conformers, implying substantial loop flexibility but overall conserved parallel topology. [12,16].

2.3. Peroxidase Activities of G-Quadruplex Split Fragments

To identify optimal split positions for biosensor design, we evaluated two split strategies (2:2 and 3:1) for the four G-quadruplex (G4) DNAzymes (Bcl2, C-myc, PS5.M, and C-kit). Figures 3–6 show the sequences of the 2:2 split (e.g., Bcl2/A and Bcl2/B) and the 3:1 split (e.g., Bcl2/C and Bcl2/D) for each DNAzyme. Each fragment pair was tested at 0.125 μM DNAzyme concentration in ABTS/H_2O_2 assays (5 mM H_2O_2, 1 mM ABTS), monitoring A_{415} for 600 s. Ideally, suitability requires near-zero activity for individual fragments in the OFF-state. Since leakage is context dependent [17], we defined OFF-state leakage as fragment activity ≥10–20% of intact DNAzyme activity at 600 s.

Bcl2 (Figure 3)**:** The intact Bcl2 DNAzyme showed strong activity (A_{415} = 0.211 at 600 s). In the 2:2 split, Bcl2/A retained nearly full activity (0.196), while Bcl2/B reached 0.059, indicating substantial OFF-state leakage. Thus, this split is unsuitable for biosensing. The 3:1 split improved performance: Bcl2/C remained at baseline, but Bcl2/D reached 0.112, about half of the intact DNAzyme's activity. While background was reduced compared to 2:2, only one fragment met the OFF-silent criterion.

C-myc (Figure 4)**:** The intact C-myc exhibited the highest activity among all sequences (A_{415} = 0.365 at 600 s). In the 2:2 split, C-myc/A plateaued at 0.119 and C-myc/B at 0.080, confirming both fragments retained significant activity. The 3:1 split reduced leakage slightly: C-myc/C reached 0.077 and C-myc/D, 0.1 at 600 s. Despite this improvement, neither split produced OFF-silent fragments.

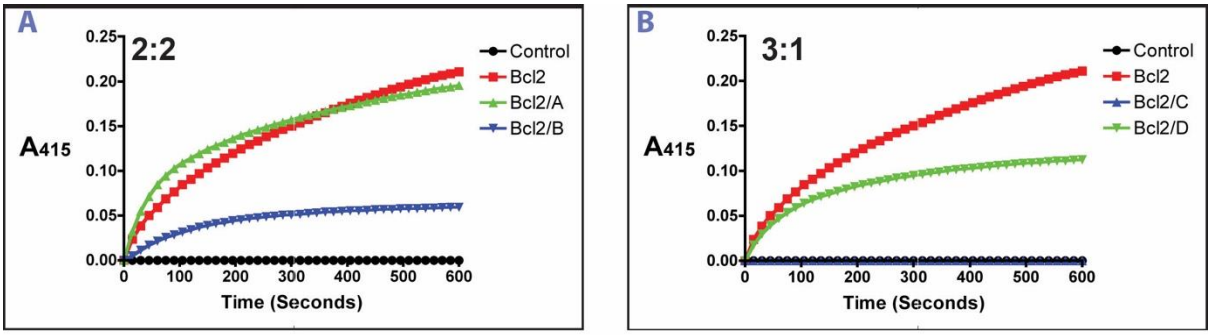

Bcl2/A 5′-GGGCGCGGGAG-3′
Bcl2/B 5′-GAAGGGGGCGGG-3′

Bcl2/C 5′-GGGCGC-3′
Bcl2/D 5′-GGGAGGAAGGGGGCGGG-3′

Figure 3. Peroxidase activities of Bcl2, and its split fragments. (**A**) 2:2 split (Bcl2/A and Bcl2/B). (**B**) 3:1 split (Bcl2/C and Bcl2/D). Catalytic activities were determined at 25 °C using ABTS/H_2O_2 oxidation. The peroxidase activity of each DNAzyme was determined at 0.125 μM DNA using 1 mM ABTS, and 5 mM H_2O_2 as described in the Methodology section. Absorbance at 415 nm (A_{415}) was monitored every 5 s for 600 s. Control reactions contain 1 μM hemin in place of the DNA/hemin complex. The sequences of the split sequences are as shown.

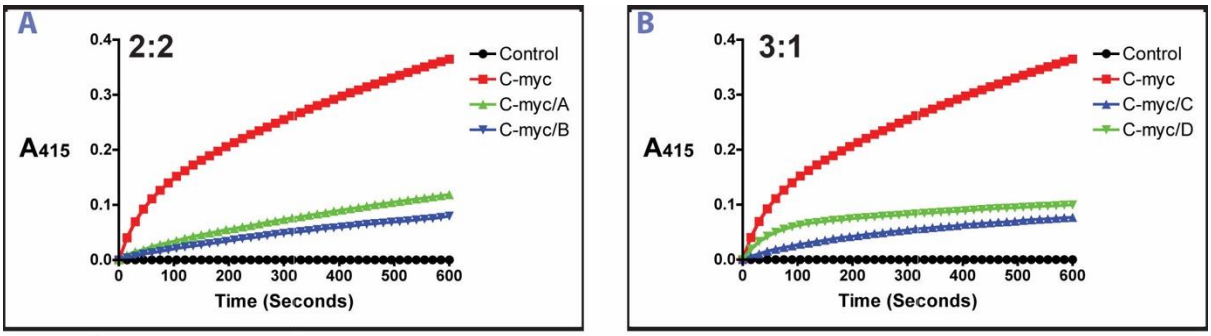

C-myc/A 5′-GAGGGTGGGGA-3′
C-myc/B 5′-GGGTGGGGAAG-3′

C-myc/C 5′-GAGGGTGGGGAGGGT-3′
C-myc/D 5′-GGGGAAG-3′

Figure 4. Peroxidase activities of C-myc, and its split fragments. (**A**) 2:2 split (C-myc/Aand C-myc/B). (**B**) 3:1 split (C-myc/C and C-myc/D). Catalytic activities were determined at 25 °C using ABTS/H_2O_2 oxidation. The peroxidase activity of each DNAzyme was determined at 0.125 μM DNA using 1 mM ABTS, and 5 mM H_2O_2 as described in the Methodology section. Absorbance at 415 nm (A_{415}) was monitored every 5 s for 600 s. Control reactions contain 1 μM hemin in place of the DNA/hemin complex. The sequences of the split sequences are as shown.

PS5.M (Figure 5)**:** PS5.M displayed rapid initial activity, plateauing near 0.164 by 600 s. The 2:2 split showed minimal leakage: PS5.M/A reached 0.028 and PS5.M/B 0.034, both close to the 20% threshold of full-length activity, making this configuration highly promising. The 3:1 split produced mixed results: PS5.M/C remained at baseline throughout 600 s, but PS5.M/D rose to 0.046. Thus, while asymmetry improved OFF-state performance for one fragment, the other retained moderate activity. Overall, PS5.M offers the most favorable split pattern among the tested sequences.

C-kit (Figure 6)**:** The intact C-kit reached $A_{415} \approx 0.16$ at 600 s. In the 2:2 split, C-kit/A plateaued near 0.11 and C-kit/B near 0.06, indicating high leakage. The 3:1 split suppressed activity in C-kit/D (~0.01), but C-kit/C remained strongly active (~0.11), similar to C-kit/A. Consequently, neither split strategy produced fully OFF-silent fragments, though engineering the leaky fragment may improve suitability.

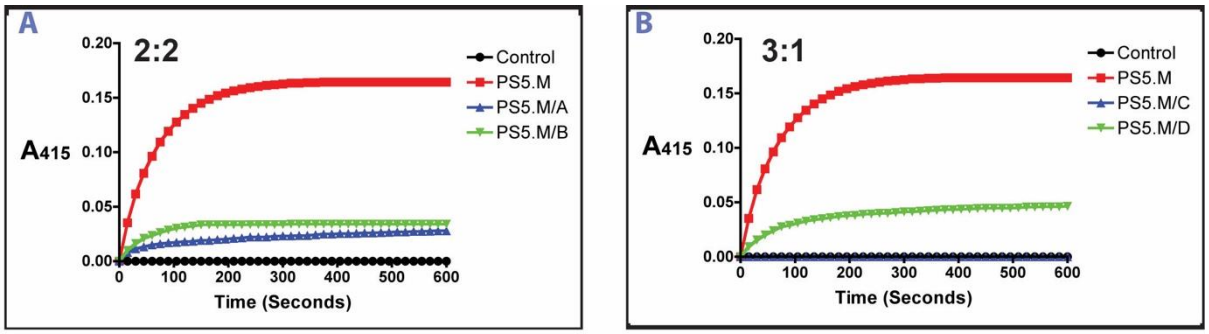

PS5.M/A 5′-GTGGGTCATTGTGGT-3′
PS5.M/B 5′-GGGTGTGG-3′
PS5.M/C 5′-GTGGGTCAT-3′
PS5.M/D 5′-TGTGGTGGGTGTGG-3′

Figure 5. Peroxidase activities of PS5.M, and its split fragments. (**A**) 2:2 split (PS5.M/A and PS5.M/B). (**B**) 3:1 split (PS5.M/C and PS5.M/D). Catalytic activities were determined at 25 °C using ABTS/H_2O_2 oxidation. The peroxidase activity of each DNAzyme was determined at 0.125 µM DNA using 1 mM ABTS, and 5 mM H_2O_2 as described in the Methodology section. Absorbance at 415 nm (A_{415}) was monitored every 5 s for 600 s. Control reactions contain 1 µM hemin in place of the DNA/hemin complex. The sequences of the split sequences are as shown.

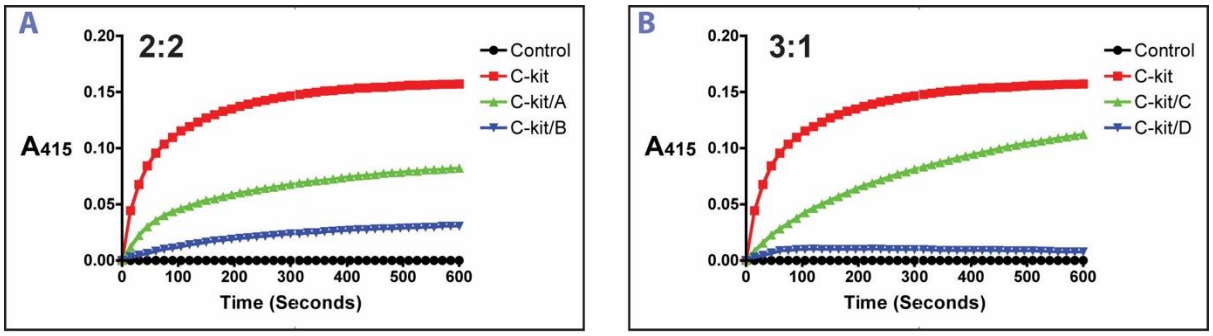

C-kit/A 5′-CGGGCGGGCGCGA-3′
C-kit/B 5′-GGGAGGGG-3′
C-kit/C 5′-CGGGCGGGCGCGAGGG-3′
C-kit/D 5′-AGGGG-3′

Figure 6. Peroxidase activities of C-kit, and its split fragments. (**A**) 2:2 split (C-kit/A and C-kit/B). (**B**) 3:1 split (C-kit/C and C-kit/D). Catalytic activities were determined at 25 °C using ABTS/H_2O_2 oxidation. The peroxidase activity of each DNAzyme was determined at 0.125 µM DNA using 1 mM ABTS, and 5 mM H_2O_2 as described in the Methodology section. Absorbance at 415 nm (A_{415}) was monitored every 5 s for 600 s. Control reactions contain 1 µM hemin in place of the DNA/hemin complex. The sequences of the split sequences are as shown.

Table 2 shows a summary of the A_{415} values (at 600 s), percentage leakage of the split fragments relative to the parent G-4 DNAzymes, the signal-to-leakage (S/L) ratio, and a quantitative classification describing if the split pair is acceptable or unacceptable for use in biosensor development.

Table 2. Endpoint activities (at 600 s), percentage leakage, signal/leakage (S/L) ratios, and quantitative classifications of G-4 DNAzymes and split fragments.

Scaffold/Variant	A_{415} @ 600 s (Mean ± SD)	Leakage (% of Bcl2)	S/L Ratio (Bcl2/Variant)	Qualitative Classification
Bcl2				
Bcl2 (intact)	0.211 ± 0.005	–	–	Baseline
Bcl2/A (2:2)	0.196 ± 0.001	92.9%	1.08	Unacceptable
Bcl2/B (2:2)	0.059 ± 0.004	28.1%	3.56	Unacceptable
Bcl2/C (3:1)	0.000 ± 0.000	0.0%	∞	Acceptable
Bcl2/D (3:1)	0.112 ± 0.003	53.2%	1.88	Unacceptable

Table 2. *Cont.*

Scaffold/Variant	A_{415} @ 600 s (Mean ± SD)	Leakage (% of Bcl2)	S/L Ratio (Bcl2/Variant)	Qualitative Classification
C-myc				
C-myc (intact)	0.365 ± 0.025	–	–	Baseline
C-myc/A (2:2)	0.119 ± 0.003	32.5%	3.08	Unacceptable
C-myc/B (2:2)	0.080 ± 0.002	21.8%	4.58	Unacceptable
C-myc/C (3:1)	0.077 ± 0.000	21.1%	4.74	Unacceptable
C-myc/D (3:1)	0.100 ± 0.005	27.3%	3.66	Unacceptable
PS5.M				
PS5.M (intact)	0.164 ± 0.006	–	–	Baseline
PS5.M/A (2:2)	0.028 ± 0.002	17.0%	5.87	Unacceptable (strict ≤10%) Borderline (under ≤20%)
PS5.M/B (2:2)	0.034 ± 0.000	20.7%	4.83	Unacceptable (strict ≤10%) Borderline (about ≤20%)
PS5.M/C (3:1)	0.000 ± 0.000	0.0%	∞	Acceptable
PS5.M/D (3:1)	0.046 ± 0.002	28.2%	3.55	Unacceptable
C-kit				
C-kit (intact)	0.157 ± 0.007	–	–	Baseline
C-kit/A (2:2)	0.082 ± 0.002	52.3%	1.91	Unacceptable
C-kit/B (2:2)	0.031 ± 0.003	19.5%	5.13	Unacceptable (strict ≤10%) Borderline (under ≤20%)
C-kit/C (3:1)	0.112 ± 0.003	71.4%	1.40	Unacceptable
C-kit/D (3:1)	0.008 ± 0.002	4.9%	20.52	Acceptable

Overall, the results show that PS5.M (2:2 split) has the best performance, with both fragments showing activities within the acceptable range. Bcl2 (3:1 split) showed a moderate performance, one fragment silent, the other moderately active. In contrast, C-myc and C-kit were least desirable, showing strong leakage in all splits due to stable G4 folding (Table 2).

3. Discussion

3.1. Sequence-Specific Activities of G4-Quadruplex DNAzymes

An analysis of the dynamic range and linearity of the reactions (Figure 2; Table 1) shows that C-myc and Bcl2 display near-proportional increases with DNAzyme concentration over the range tested, a feature that could be advantageous for quantitative sensing. It is essential to note that the performance of these split systems can only be verified for biosensing purpose upon characterization of their activities in reactions where the target probe is included. PS5.M and C-kit show early saturation, which can potentially compress dynamic range at longer readouts [12]. In terms of time-to-signal ratio, PS5.M and C-kit gave fast ON signals with steep early slopes. These features are useful for designing rapid, true/false assays with short read windows. In contrast, C-myc displayed both fast onset and continuing growth, while Bcl2 reactions are slower initially but catch up over the course of the reactions. When considering signal stability, the minimal decay or curvature for C-myc suggests greater catalytic stability in these conditions. PS5.M and C-kit show early saturation, consistent with the known vulnerability of some G4/hemin systems to oxidative inactivation [12].

Careful consideration of the peroxidase activities of the four GQs at the three concentrations suggests three principles that explain the observed trends. (i) The first is the topology state of each GQ. Parallel G4s present an accessible 3′-terminal G-tetrad that preferentially stacks hemin and tends to show higher peroxidase activities than antiparallel folds; C-myc and Bcl2 fit this profile and outperform at 600 s [11,13]. (ii) The second principle is the effect of adjacent bases in tuning catalysis. It is known that 3′-adjacent

adenines can act as distal-histidine mimics to accelerate compound-I formation and promote higher activity. This effect is general across parallel G4s and a practical consideration for biosensor design [2]. (iii) The final point is the kinetic susceptibility of the DNAzyme under peroxidation conditions. G4/hemin complexes can self-inactivate in the presence of high H_2O_2 concentrations, leading to burst-and-plateau kinetics (as for PS5.M and C-kit). Buffer composition and additives can be optimized to mitigate this effect. For example, NH_4^+ or polyamines can enhance stability and reaction velocity [12,18].

3.2. Suitability of G4-Quadruplex DNAzymes for Use in Biosensing Applications

A key requirement of split designs is the ability to reconstruct an active G4 complex upon recognition and binding to an analyte. The data shown in Figure 2 when analyzed with information available from the literature allow us to draw the following guiding principles on each of the four GQs we studied.

C-myc appears to be the best overall system to use as a starting point in designing a split system. This is supported by its high and sustained activity, good concentration linearity, and a parallel topology known to tolerate effective 1:3 or 2:2 splits. It is anticipated that including short flanking d(TC) on one arm or d(ATT) within a loop can raise the signal in split formats by adding a 3′-adjacent Adenine next to the hemin-binding face, which further boosts activity [2,8]. **Bcl2** shows robust, sustained peroxidase activity, and is likely to give reliable quantitative readouts. It has been shown to respond well to multimerization, which has shown synergistic rate gains for parallel scaffolds [7,11].

C-kit reactions are characterized by a fast increase in activities but are more likely to reach saturation early. It could be useful where rapid detection is desired and readout windows are short. Its activity can be enhanced by dimeric/zippered or covalent hemin strategies. Structural evidence shows it maintains conserved parallel folds with flexible loops, which may help in reassembly of split parts, but may favor early saturation in ABTS assays [9,16].

PS5.M reactions are characterized by strong initial rates, but like C-kit, it is vulnerable to early saturation. Hence, it could be less ideal for quantitative split sensors unless mitigating conditions are built in to tune the system. Addition of modulating substances (e.g., spermine or NH_4^+) can partially enhance the activity. Alternatively, the pronounced burst of activity can be adapted for rapid qualitative assays [7,18].

Overall, the observed hierarchy (C-myc $\geq$ PS5.M $\geq$ c-Kit > Bcl2) matches expectations from G4 topology and terminal-quartet chemistry. Parallel motifs with accessible 3′ quartets typically support faster catalysis, and adjacent adenine near the 3′ quartet can further accelerate turnover. C-myc is therefore the strongest candidate when maximal sensitivity is required. PS5.M and c-Kit provide faster onset (short T_{50}), advantageous for rapid assays. Bcl2 reaches a high endpoint but exhibits slower early-phase accumulation, consistent with polymorphic folding.

3.3. Suitability of the Tested Split Pairs for Construction of Biosensing Gates

Designing split G-quadruplex (G4) DNAzymes for biosensors requires fragments that remain catalytically silent in the absence of target, ensuring high ON/OFF ratios and minimal background. Our analyses highlight significant differences in split performance across the four G4 scaffolds we tested (Bcl2, C-myc, PS5.M, and C-kit) reflecting their intrinsic folding propensities and structural features (Figures 3–6).

Bcl2: The 2:2 split (Bcl2/A and Bcl2/B) is unsuitable because Bcl2/A retains nearly full activity and Bcl2/B is not silent, producing high background that would obscure a target-dependent signal. The 3:1 split (Bcl2/C and Bcl2/D) performs better: Bcl2/C is OFF-silent, but Bcl2/D retains ~50% activity, still causing leakage. The observed activity profile

observed for the split Bcl2 fragments agrees with demonstrated G-quadruplex/hemin pattern [7,11]. Bcl2/D retains multiple G-tracts and may provide an accessible 3′ terminal tetrad for hemin stacking and catalytic competence. The proximal A/C nucleobases near the 3′ stacking site can further accelerate H_2O_2 activation, potentially explaining the strong activity. In contrast, Bcl2/C (5′-GGGCGC) is too short and does not contain sufficient G-tracts to form a competent G-quadruplex alone; hence its activity did not rise beyond baseline. To optimize Bcl2, splits should partition G-tracts so neither fragment forms a G4 independently ($\leq$2 weakened tracts per fragment), or sequence edits (e.g., GGG to GG, G to A/T substitutions, short spacers) should reduce intrinsic G4 propensity. These modifications would allow fragments to reconstitute an active G4 only upon target-mediated assembly.

C-myc: This DNAzyme forms a highly stable parallel G4 with short loops [19], making OFF-silent splits and making truncated fragments prone to folding. Both tested strategies (2:2 and 3:1) leave fragments with multiple GGG tracts and favorable flanking bases, enabling autonomous G4 folding and hemin binding. Consequently, all fragments exhibit strong leakage, and ON/OFF ratios remain poor. The extended, non-saturating activity profiles suggest continued accumulation of active complexes or slow inactivation. Effective optimization would require adopting non-classical splits such as cutting within loops or introducing destabilizing edits to suppress spontaneous folding while preserving target-driven assembly. Splits that leave three or more contiguous guanines plus favorable flanking bases allow partial G4 formation and hemin binding. Both C-myc/A and C-my/B preserve multiple GGG tracts, potentially enabling intramolecular G4 formation or concentration-facilitated multimeric G4 assembly with an accessible terminal G-tetrad (often the 3′ face) for hemin stacking [2], yielding robust peroxidase-mimicking activity without a target. Similarly, C-my/C retains multiple GGG tracts, which could enable intramolecular G-quadruplex formation or concentration-assisted tetramolecular/multimeric assembly with an accessible terminal G-tetrad for hemin stacking, accounting for the observed measurable catalysis. The other split fragment, C-myc/D, although short (5′-GGGGAAG), contains GGGG, which may participate in tetramolecular parallel G4s [20], hence the observed activity.

PS5.M: PS5.M exhibits robust DNAzyme activity but lower per-molecule rates than parallel G4s due to its non-parallel conformations and less optimal terminal tetrads. The 2:2 split (PS5.M/A and PS5.M/B) is promising: both fragments are essentially silent, satisfying OFF-state requirements. The 3:1 split (PS5.M/C and PS5.M/D) is partially suitable: PS5.M/C is OFF-silent, but PS5.M/D retains moderate activity (~0.045), likely due to residual G-tract integrity. Redesign strategies including non-classical splits, loop/flank edits, and template-assisted assembly could yield fully silent fragments that reconstitute efficiently upon target binding. These findings agree with general split G4 rules that disrupting G-tracts and avoiding exposed terminal tetrads are key to suppressing OFF-state catalysis.

C-kit: For C-kit, both split strategies tested (2:2 and 3:1) fail to produce OFF-silent fragments. The observed strong leakage in the C-kit split pairs can be accounted for by the predicted tendency of the C-kit sequence to form a stable G4 with multiple contiguous G-tracts [10], making even truncated fragments prone to folding. As discussed for Bcl2 and C-myc above, splits that leave three or more contiguous guanines and having favorable flanking bases may support partial G4 formation and hemin binding. C-kit/C evidently retains sufficient G-tract content/registry and an accessible terminal G-tetrad (and possibly supportive proximal bases) to form a catalytically competent G4/hemin complex on its own. C-kit/D (5′-AGGGG) lacks the tract architecture required for autonomous folding into an active G4 under these conditions, hence its lack of activity. Achieving OFF-silent

fragments would require radical redesign, such as deep tract partitioning or destabilizing edits, to prevent autonomous G4 formation.

Split G-quadruplex DNAzyme design hinges on achieving OFF-silent fragments to ensure high ON/OFF ratios and low background. Among the tested sequences, PS5.M offers the most promising scaffold for split-based biosensors, while Bcl2 can be optimized through tract partitioning and sequence weakening. To be useful for designing biosensors, C-myc and C-kit will require radical split redesign strategies. Intact C-myc and Bcl2 exhibit high catalytic activities, but their split fragments retained activities in the OFF-state. Asymmetric splits generally reduce background compared to symmetric splits, but success depends on fragment tract integrity [21,22]. These findings provide a rational basis for selecting scaffolds and split strategies for biosensor development. In addition, our findings underscore the importance of rational split positioning, tract integrity disruption, and sequence engineering in developing reliable G-quadruplex-based biosensing platforms.

Recent studies have explored non-classical split approaches with the aim of optimizing the performance of G4-DNAzyme biosensors. Zhu et al. [21] investigated six different split modes for the G4-forming sequence T30695 (GGGTGGGTGGGTGGGT) and concluded that the 4:8 split gave the highest signal-to-background ratio in fluorescence assays. This split mode was found to minimize background fluorescence due to the specific interactions of the G-rich segments, which enhances the sensitivity of the assay. Although the analysis is limited to a single G4 sequence, the findings could be extended to other systems such as the ones studied here. It is also unclear how applicable the 4:8 design would be in assay systems that rely on a colorimetric signal, an essential requirement for designing low-cost biosensors for field applications. Lv et al. [4] reported that intramolecular split G4 DNAzymes use an approach different from the more common intermolecular split G4. In this design, DNA spacers are inserted into an intact G4 strand, dividing the G4 sequence into two modules linked using DNA spacer bases. It offers the opportunity of simplifying split G4 DNAzymes binary probes into a single probe. The results show that intra-SG designs could offer more traditional stability than the classical intermolecular systems.

It is noteworthy that while these alternative split approaches offer some advantages as stated above, the choices of the G4 sequence and split sites remain context dependent. For example, Connelly et al. [17] reported that the primary and/or secondary structure of the target could significantly affect the performance of the probe, and that unintended interactions between the target and its recognition sites are observed especially in cytosine-rich targets.

3.4. Design Implications and Approaches to Design Leak-Proof Split G-Quadruplexes

The results from this study align with the broader consensus that parallel G4s and designs enhancing 3′ hemin stacking or distal histidine-like interactions yield the most robust signals [2,3,23]. However, careful tract partitioning and sequence engineering remain essential for minimizing leakage in split systems. By integrating kinetic analysis with split-mode evaluation, this study provides actionable design principles for G4 DNAzyme biosensors, enabling applications in quantitative diagnostics, rapid screening, and programmable molecular logic.

Our findings reveal that designing leak-proof split G-quadruplex (G4) DNAzymes remains challenging due to the intrinsic requirements for catalytic activity. Since leakage is context dependent [17], we defined OFF-state leakage as fragment activity $\geq$10–20% of intact DNAzyme activity at 600 s. Hemin–G4 complexes rely on an exposed terminal G-tetrad for stacking and adjacent bases (e.g., A/C) that act as proton relays or distal ligands, enhancing peroxidase-like catalysis [3,6]. Parallel G4s with accessible 3′ tetrads are particularly efficient, but this structural advantage also predisposes fragments to residual

activity when split. For example, Bcl2 fragments Bcl2/A and Bcl2/D retained significant activity because classical splits preserved long contiguous G-runs and favorable loop contexts. This observation agrees largely with previous reports that symmetric splits (6:6 or 2:2) and asymmetric split (9:3 or 3:1) often leak, whereas non-classical partitions disrupting tract integrity (e.g., 2:10, 4:8, 5:7) markedly reduce spontaneous folding [4,8]. Loop and flanking nucleotides further modulate OFF-state activity by influencing hemin binding and proton transfer microenvironments. The patterns obtained from the 2:2 and the 3:1 split example studied here lay the foundation for their potential use in designing biosensors. It is necessary to emphasize that the performance of these systems remain context dependent since the sequence of the target probe could play a significant part in determining how applicable these sequence-specific designs are [17].

Several strategies can mitigate leakage without compromising ON-state performance: (i) Non-classical splits that interrupt consecutive G-tracts in both fragments to suppress autonomous folding [4]. (ii) Destabilizing the long fragment by inserting short non-G spacers or relocating catalytic loop adenines to weaken OFF-state activity while preserving target-driven assembly [8]. (iii) Flanking sequence control, such as removing 3′ adenines/cytosines near the hemin-binding tetrad in isolated fragments and restoring them via helper strands upon assembly [3]. (iv) Template-assisted proximity assembly, using duplex or junction-based architectures to enforce conditional activation [5,24].

PS5.M demonstrated the most promising split behavior, with PS5.M/C (short fragment in 3:1 split) remaining completely silent. Optimizing this scaffold could involve weakening PS5.M/D through non-classical repartition or loop/flank edits until both fragments meet OFF-state criteria.

Overall, these insights underscore that rational split design requires balancing tract disruption, sequence engineering, and assembly strategies to achieve ultra-low leakage while maintaining strong ON-state activity. Future work should integrate these principles with proximity-driven architectures and chemical modifications to advance robust split DNAzyme biosensors. We acknowledge that the reasonings above assume that the DNAzyme sequences and split fragments retain the parallel G4 topology. The proposed modifications will need to be validated alongside structural characterization of any new constructs.

4. Materials and Methods

4.1. Experimental Design Rationale

This study was designed to address two key objectives for developing split G-quadruplex (G4) DNAzyme biosensors: (i) to compare the catalytic properties of commonly used G4 scaffolds under standardized conditions, and (ii) to evaluate whether these scaffolds can be split into fragments that remain OFF-silent on their own without residual peroxidase activities. The potential peroxidase activities of split fragment pairs that meet this criterion can be activated through target-induced assembly. Four representative sequences—C-myc, Bcl2, PS5.M, and C-kit—were selected to cover both parallel and non-parallel topologies. Each intact DNAzyme was characterized for peroxidase-like activity using ABTS/H_2O_2 oxidation kinetics. Two split strategies (2:2 symmetric and 3:1 asymmetric) were tested for each scaffold to assess OFF-state leakage and ON-state potential. This systematic approach enables identification of scaffolds and design principles that minimize background activity while preserving a strong target-dependent signal, providing a rational basis for engineering robust split DNAzyme biosensors.

4.2. Materials

HPLC-purified synthetic DNA oligonucleotides corresponding to intact G4 sequences and their split fragments were purchased from Integrated DNA Technologies (IDT). Hemin (≥95%), ABTS, and hydrogen peroxide (H_2O_2, 30%) were obtained from Sigma-Aldrich. All other reagents used were obtained from Fisher Scientific UK and were of analytical grade unless otherwise specified. Oligonucleotides were dissolved in TE buffer (10 mM Tris-HCl pH 7.5, 0.1 mM EDTA) as 100 μM solutions and verified using A_{260} to ensure consistency across all G4 sequences and their split fragments and stored at −20 °C until when needed for reactions.

4.3. Methods

DNAzyme Folding and Hemin Complexation: Oligonucleotides were complexed to hemin to obtain a catalytic unit (DNAzyme) with peroxidase activity. Briefly, 50 μL of 100 μM oligonucleotide solution in TE (1×) was added to 450 μL of a buffer that contains 25 mM Tris-HCl pH 7.4, 20 mM KCl, 200 mM NaCl, 0.05% Triton X-100, 1% DMSO. The oligonucleotide samples were heated at 95 °C for 10 min and cooled rapidly at 0 °C by dipping it into ice for 15 min. It was later kept at 25 °C for 15 min to attain the higher-ordered structure that is needed to bind hemin to form a DNA–hemin complex. To assemble the catalytic complex, a 5 μL sample of 100 μM hemin solution was added to 245 μL of 10 μM folded oligonucleotide; the resultant solution was mixed properly and was kept at 25 °C for 30 min to allow the formation of an oligonucleotide–hemin complex. The resultant solution gives 10 μM DNAzymes.

Split Design: Two split strategies were evaluated for each G4 scaffold: (i) Symmetric split (2:2): G-tracts divided evenly between fragments. (ii) Asymmetric split (3:1): One fragment contains three G-tracts, the other one tract. Sequences were selected to preserve loop architecture where possible. Split fragments were tested individually and as reconstituted pairs.

Peroxidase Activity Assay: The activities of the G4-DNAzymes were determined in 500 μL reactions that contained 25 mM HEPES-NaOH pH 7.4, 20 mM KCl, 200 mM NaCl, 0.05% Triton X-100, 1% DMSO, DNAzyme (0.025–0.125 μM), ABTS (1 mM), and H_2O_2 (5 mM). Each reaction was started by the addition of H_2O_2, and change in A_{415} (characteristic for the reaction product $ABTS^{\bullet}$) was monitored immediately after starting the reaction every 5 s over 5 min on a CLARIOstar Plate Reader (BMG LABTECH, Ortenberg, Germany). All reactions were carried out at 25 °C, consistent with previous studies on peroxidase DNAzyme reaction [1,7,14,15].

Data Analysis: Each condition was tested in triplicate. Mean A_{415} values and standard deviations were plotted as kinetic curves. OFF-state leakage was defined as fragment activity ≥10–20% of intact DNAzyme activity at 600 s. Suitability for biosensing was assessed based on the ON/OFF ratio and signal-to-background performance.

For the kinetic analysis data reported in Figure 2, raw absorbance traces at 415 nm ($ABTS^{\bullet+}$ readout) were exported for each DNAzyme at 0.025, 0.05, and 0.125 μM with three technical replicates per condition and matched hemin-only controls. At every time point, replicate signals were baseline-subtracted by the time-matched mean of the control replicates. For each replicate, an initial rate (Abs s^{-1}) was obtained by ordinary least-squares linear regression of A(t) over 0–120 s (inclusive). The mean and standard error of the mean (SEM) were computed across the three replicates. The endpoint signal was defined as the baseline-subtracted absorbance at 600 s. Time-to-half-maximum (T_{50}) was calculated by linear interpolation to the time at which the baseline-subtracted mean curve first reached 50% of its final value.

Design Optimization Criteria: Fragments showing residual activity were analyzed for tract continuity and flanking sequence composition. Strategies for leakage suppression included non-classical splits, insertion of non-G spacers, loop/flank edits, and template-assisted assembly designs [3,4,8,17].

5. Conclusions and Future Prospects

Split G-quadruplex DNAzyme design hinges on achieving OFF-silent fragments to ensure high ON/OFF ratios and low background. Among the tested sequences, PS5.M offers the most promising scaffold for split-based biosensors based on OFF-state performance, while Bcl2 can be optimized through tract partitioning and sequence weakening. In contrast, C-myc and C-kit, due to their strong intrinsic G4 stability, demand radical redesign strategies. These findings underscore the importance of rational split positioning, tract integrity disruption, and sequence engineering in developing reliable G-quadruplex-based biosensing platforms.

Our results establish a selection of design opportunities for split G4 DNAzymes: PS5.M for stringent OFF suppression, Bcl2 for durable read windows, C-myc for near-linear quantitation, and C-kit for segmented, binary outputs. To achieve these potential applications, mechanistic modeling that integrates G4 folding, hemin binding, and inactivation should enable predictive selection of DNAzyme sequences, split sites, and appropriate buffers. OFF-silencing can be advanced via non-classical partitions, loop/flank edits, and target-templated clamps, complemented by kinetic gating (toeholds, hairpin sequestration). The application of experimental data for these well-studied G4 sequences will allow development of sensitive and portable biosensors. On a broader scope, standards for benchmarking and high-throughput, data-driven optimization will accelerate iteration, moving split G4 DNAzymes toward robust, deployable, programmable biocatalysts.

Author Contributions: Conceptualization, D.S.O. and F.J.O.; methodology, R.I.A., D.S.O. and F.J.O.; software, D.S.O. and F.J.O.; validation, F.J.O.; formal analysis, D.S.O. and F.J.O.; investigation, D.S.O.; resources, R.I.A., D.S.O., F.J.O. and S.O.M.; data curation, D.S.O.; writing—original draft preparation, R.I.A., D.S.O. and F.J.O.; writing—review and editing, R.I.A., D.S.O. and F.J.O.; visualization, D.S.O. and F.J.O.; supervision, F.J.O. and S.O.M.; project administration, F.J.O. and S.O.M.; funding acquisition, F.J.O. All authors have read and agreed to the published version of the manuscript.

Funding: This research was supported by institutional funding from Liverpool John Moores University, Liverpool, UK.

Data Availability Statement: Data are contained within the article.

Conflicts of Interest: The authors declare no conflicts of interest.

References

1. Travascio, P.; Li, Y.; Sen, D. DNA-Enhanced Peroxidase Activity of a DNA Aptamer-Hemin Complex. *Chem. Biol.* **1998**, *5*, 505–517. [CrossRef]
2. Li, W.; Li, Y.; Liu, Z.; Lin, B.; Yi, H.; Xu, F.; Nie, Z.; Yao, S. Insight into G-Quadruplex-Hemin DNAzyme/RNAzyme: Adjacent Adenine as the Intramolecular Species for Remarkable Enhancement of Enzymatic Activity. *Nucleic Acids Res.* **2016**, *44*, 7373–7384. [CrossRef]
3. Cao, Y.; Ding, P.; Yang, L.; Li, W.; Luo, Y.; Wang, J.; Pei, R. Investigation and Improvement of Catalytic Activity of G-Quadruplex/Hemin DNAzymes Using Designed Terminal G-Tetrads with Deoxyadenosine Caps. *Chem. Sci.* **2020**, *11*, 6896–6906. [CrossRef]
4. Lv, M.; Guo, Y.; Ren, J.; Wang, E. Exploration of Intramolecular Split G-Quadruplex and Its Analytical Applications. *Nucleic Acids Res.* **2019**, *47*, 9502–9510. [CrossRef]
5. Ida, J.; Kuzuya, A.; Choong, Y.S.; Lim, T.S. An Intermolecular-Split G-Quadruplex DNAzyme Sensor for Dengue Virus Detection. *RSC Adv.* **2020**, *10*, 33040–33051. [CrossRef]

6. Shumayrikh, N.; Sen, D. Heme•G-Quadruplex DNAzymes: Conditions for Maximizing Their Peroxidase Activity. In *G-Quadruplex Nucleic Acids: Methods and Protocols*; Springer: New York, NY, USA, 2019; pp. 357–368. [CrossRef]
7. Adeoye, R.I.; Osalaye, D.S.; Ralebitso-Senior, T.K.; Boddis, A.; Reid, A.J.; Fatokun, A.A.; Powell, A.K.; Malomo, S.O.; Olorunniji, F.J. Catalytic Activities of Multimeric G-Quadruplex Dnazymes. *Catalysts* **2019**, *9*, 613. [CrossRef]
8. Connelly, R.P.; Fonseca, V.; Gerasimova, Y.V. Peroxidase-like Activity of G-Quadruplex/Hemin Complexes for Colorimetric Nucleic Acid Analysis: Loop and Flanking Sequences Affect Signal Intensity. *DNA* **2025**, *5*, 12. [CrossRef]
9. Li, J.; Wu, H.; Yan, Y.; Yuan, T.; Shu, Y.; Gao, X.; Zhang, L.; Li, S.; Ding, S.; Cheng, W. Zippered G-Quadruplex/Hemin DNAzyme: Exceptional Catalyst for Universal Bioanalytical Applications. *Nucleic Acids Res.* **2021**, *49*, 13031–13044. [CrossRef]
10. Kuryavyi, V.; Phan, A.T.; Patel, D.J. Solution Structures of All Parallel-Stranded Monomeric and Dimeric G-Quadruplex Scaffolds of the Human c-Kit2 Promoter. *Nucleic Acids Res.* **2010**, *38*, 6757–6773. [CrossRef]
11. Liu, B.; Li, D.; Shang, H. General Peroxidase Activity of a Parallel G-Quadruplex-Hemin DNAzyme Formed by Pu39WT-a Mixed G-Quadruplex Forming Sequence in the Bcl-2 P1 Promoter. *Chem. Cent. J.* **2014**, *8*, 43. [CrossRef]
12. Monte Carlo, A.R., III; Fu, J. Inactivation Kinetics of G-Quadruplex/Hemin Complex and Optimization for More Reliable Catalysis. *Chempluschem* **2022**, *87*, e202200090. [CrossRef]
13. Cao, Y.; Li, W.; Pei, R. Exploring the Catalytic Mechanism of Multivalent G-Quadruplex/Hemin DNAzymes by Modulating the Position and Spatial Orientation of Connected G-Quadruplexes. *Anal. Chim. Acta* **2022**, *1221*, 340105. [CrossRef]
14. Stefan, L.; Denat, F.; Monchaud, D. Insights into How Nucleotide Supplements Enhance the Peroxidase-Mimicking DNAzyme Activity of the G-Quadruplex/Hemin System. *Nucleic Acids Res.* **2012**, *40*, 8759–8772. [CrossRef]
15. Adeoye, R.I.; Ralebitso-Senior, T.K.; Boddis, A.; Reid, A.J.; Giuntini, F.; Fatokun, A.A.; Powell, A.K.; Ihekwaba-Ndibe, A.; Malomo, S.O.; Olorunniji, F.J. Spermine Enhances the Peroxidase Activities of Multimeric Antiparallel G-Quadruplex DNAzymes. *Biosensors* **2025**, *15*, 12. [CrossRef]
16. Wei, D.; Husby, J.; Neidle, S. Flexibility and Structural Conservation in a C-KIT G-Quadruplex. *Nucleic Acids Res.* **2015**, *43*, 629–644. [CrossRef]
17. Connelly, R.P.; Verduzco, C.; Farnell, S.; Yishay, T.; Gerasimova, Y.V. Toward a Rational Approach to Design Split G-Quadruplex Probes. *ACS Chem. Biol.* **2019**, *14*, 2701–2712. [CrossRef]
18. Zhang, X.; Zhu, C.; Wang, Y.; Zhao, Y.; Tang, H.; Li, X.; Wu, P. Impact of NH4+ on the Catalytic Activity of G-Quadruplex/Hemin DNAzyme for Chemiluminescent Sensing. *Anal. Bioanal. Chem.* **2025**, 1–10. [CrossRef]
19. Stump, S.; Mou, T.C.; Sprang, S.R.; Natale, N.R.; Beall, H.D. Crystal structure of the major quadruplex formed in the promoter region of the human c-MYC oncogene. *PLoS ONE* **2018**, *13*, e0205584. [CrossRef]
20. Rosu, F.; Gabelica, V.; Poncelet, H.; De Pauw, E. Tetramolecular G-quadruplex formation pathways studied by electrospray mass spectrometry. *Nucleic Acids Res.* **2010**, *38*, 5217–5225. [CrossRef]
21. Zhu, J.; Zhangc, L.; Dong, S.; Wang, E. How to split a G-quadruplex for DNA detection: New insight into the formation of DNA split G-quadruplex. *Chem. Sci.* **2015**, *6*, 4822–4827. [CrossRef]
22. Li, J.; Jiang, L.; Wu, H.; Zou, Y.; Zhu, S.; Huang, Y. Self-contained G-quadruplex/hemin DNAzyme: A superior ready-made catalyst for in situ imaging analysis. *Nucleic Acids Res.* **2025**, *53*, gkaf227. [CrossRef] [PubMed]
23. Chen, J.; Zhang, Y.; Cheng, M.; Guo, Y.; Šponer, J.; Monchaud, D.; Mergny, J.L.; Ju, H.; Zhou, J. How Proximal Nucleobases Regulate the Catalytic Activity of G-Quadruplex/Hemin DNAzymes. *ACS Catal.* **2018**, *8*, 11352–11361. [CrossRef]
24. Agustin, D.F.; Vianney, Y.M.; Weisz, K.; Wahjudi, M. Structural Aspects of Split G-Quadruplexes in Quadruplex-Duplex Hybrid Systems. *ChemistrySelect* **2024**, *9*, e202304286. [CrossRef]